

Modelling earthquake ground motions by stochastic method

Nelson Lam
University of Melbourne
Australia

John Wilson
Swinburne University of Technology
Australia

Hing Ho Tsang
University of Hong Kong
China Hong Kong

1. Introduction

The prediction of earthquake ground motions in accordance with recorded observations from past events is the core business of engineering seismology. An attenuation model presents values of parameters characterising the intensities and properties of ground motions estimated of projected earthquake scenarios (which are expressed in terms of magnitude and distance). Empirical attenuation models are developed from regression analysis of recorded strong motion accelerograms. In situations where strong motion data are scarce the database of records has to cover a very large area which may be an entire continent (eg. Ambrasey model for Europe) or a large part of a continent (eg. Toro model for Central & Eastern North America) in order that the size of the database has statistical significance (Toro *et al.*, 1997; Ambrasey, 1995). Thus, attenuation modelling based on regression analysis of instrumental data is problematic when applied to regions of low and moderate seismicity. This is because of insufficient representative data that has been collected and made available for model development purposes.

An alternative approach to attenuation modelling is use of theoretical models. Unlike an empirical model, a theoretical model only makes use of recorded data to help ascertain values of parameters in the model rather than to determine trends from scratch by regression of data. Thus, much less ground motion data is required for the modelling. Data that is available could be used to verify the accuracies of estimates made by the theoretical model. Ground motion simulations by classical wave theory provides comprehensive description of the earthquake ground motions but information that is available would typically not be sufficient as input to the simulations. The heuristic source model of Brune

(1970) which defines the frequency content of seismic waves radiated from a point source is much simpler. The model has only three parameters : seismic moment, distance and the stress parameter. Combining this point source model with a number of filter functions which represent modification effects of the wave travel path and the site provides estimates for the *Fourier* amplitude spectrum of the motion generated by the earthquake on the ground surface. The source model (of Brune) in combination with the various filter functions are collectively known as the seismological model (Boore, 1983). Subsequent research by Atkinson and others provides support for the proposition that simulations from a well calibrated point source model are reasonably consistent with those from the more realistic finite fault models.

The *Fourier* spectrum as defined by the seismological model only provides description of the frequency properties of the ground motions and not the phase angles of the individual frequency components of the waveforms. Thus, details of the wave arrival times which are required for providing a complete description of the ground shaking remain uncertain as they have not been defined by the seismological model. With stochastic modelling, the pre-defined frequency content is combined with random phase angles that are generated by the *Monte Carlo* process. Thus, acceleration time-histories based on randomised wave arrival details are simulated. The simulations can be repeated many times (for the same earthquake scenario and source-path-site conditions) in order that response spectra calculated from every simulated time-histories can be averaged to obtain a smooth, ensemble averaged, response spectrum.

The seismological model has undergone continuous development since its inception in the early 1980's. For example, the original Brune source model has been replaced by the empirical source model of Atkinson (1993) which was developed from seismogram data recorded in *Central and Eastern North America* to represent conditions of intraplate earthquakes. A similar model was subsequently developed by Atkinson & Silva (2000) which was developed from data recorded in *Western North America* to represent conditions of interplate earthquakes. A model to account for the complex spread of energy in space taking into account the wave-guide phenomenon and the dissipation of energy along the wave travel path has also been developed (Atkinson & Boore, 1995). The amplification and attenuation of upward propagating waves taking into account the effects of the shear wave velocity gradient of the earth crust close to the ground surface have also been modelled by Boore & Joyner (1997).

The authors have been making use of the developing seismological model as described for constraining the frequency properties of projected earthquake scenarios for different regions around the world including regions of low-moderate seismicity where strong motion data is scarce (Chandler & Lam, 2002; Lam *et al.*, 2002, 2003, 2006, 2009; Balendra *et al.*, 2001; Yaghmaei Sabegh & Lam, 2010; Tsang *et al.*, 2010). It is typically assumed in the simulations that the intraplate source model that was originally developed for *Central and Eastern North America* is generally applicable to other intra-plate regions. Values of parameters for defining filter functions of the wave travel path could be ascertained by making references to results of seismic surveys, and in conjunction with Intensity data where necessary. Thus, earthquake ground motions that are recorded locally are not essential for model

development and time-histories simulations. Basic principles of the simulations and an introductory description of the seismological model can be found in the review article written by the authors (Lam *et al.*, 2000a). More detailed descriptions of the techniques for constraining filter functions in the absence of locally recorded ground motions can be found in Tsang & Lam (2010). Operating this modelling procedure is a very involved process. With the view of obtaining quick estimates of the response spectrum without undertaking stochastic simulations, the authors have developed a manual calculation procedure which is known as the *Component Attenuation Model* (CAM). CAM was developed from collating the experience the authors acquired in the development of response spectrum models by the stochastic procedure. The development and application of seismological modelling technique as applied to different countries, which forms the basis of CAM, has been reported in a range of journals spanning a period of ten years since 2000 (eg. Lam *et al.*, 2000a-c; Chandler & Lam, 2004; Lam & Chandler, 2005; Hutchinson *et al.*, 2003 ; Wilson *et al.*, 2003). The writing of this book chapter enables CAM to be presented in a coherent, compact, and complete manner.

2. Background to the Component Attenuation Model

A response spectrum for seismic design purposes can be constructed in accordance with parameters characterising the acceleration, velocity and displacement (*A*, *V* and *D*) demand properties of the earthquake. Response spectra presented in different formats are made up of zones representing these entities as shown in Figure 1.

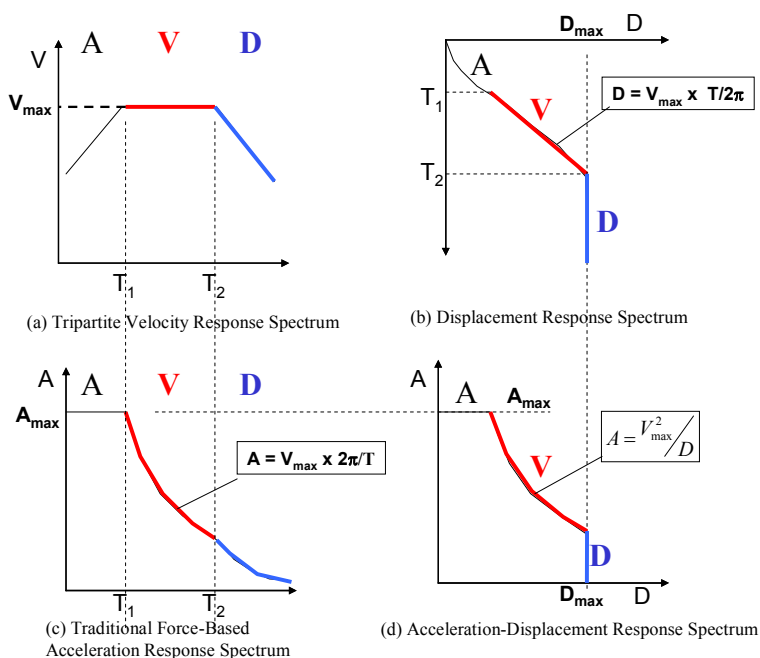


Fig. 1. Earthquake Response Spectra in different formats

The velocity response spectrum in the tri-partite format of Fig.1a in logarithmic scale is the much preferred format to use in the earthquake engineering literature given that spectral values are presented over a wide period range (eg. 0.1s - 10s) and with good resolution. Once the response spectral velocity values have been identified from the spectrum, the corresponding values of the response spectral accelerations and displacements are automatically known by means of the displayed transformation relationships. The alternative displacement response spectrum format of Fig. 1b which provides a direct indication of the drift demand of the structure in an earthquake was proposed initially by Priestley (1995) when the displacement-based approach of seismic assessment was first introduced. The acceleration-displacement response spectrum (ADRS) diagram format of Fig. 1d is also much preferred by the engineering community given that the spectral acceleration (A) values are effectively values of the base shear that have been normalised with respect to the mass of the *single-degree-of-freedom* system. Consequently, the acceleration-displacement (force-displacement) relationship of a structure can be superposed onto the ADRS diagram to identify the *performance point* which represents the estimated seismic response behaviour of the system as shown in Fig. 2. Diagrams representing seismic demand and capacity in this format are also known as the *Capacity Spectrum*. The importance of the velocity and displacement (V and D) demands as opposed to the acceleration (A) demand in the context of protecting lives and lowering the risks of overturning and collapses is evident from Figure 2 in which typical performance points associated with ultimate behaviour of the structure are shown.

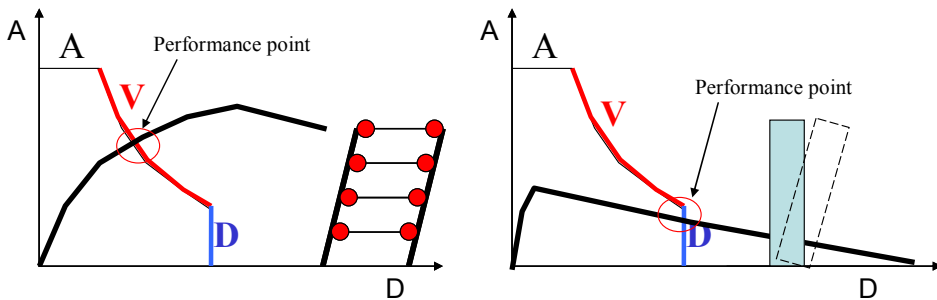


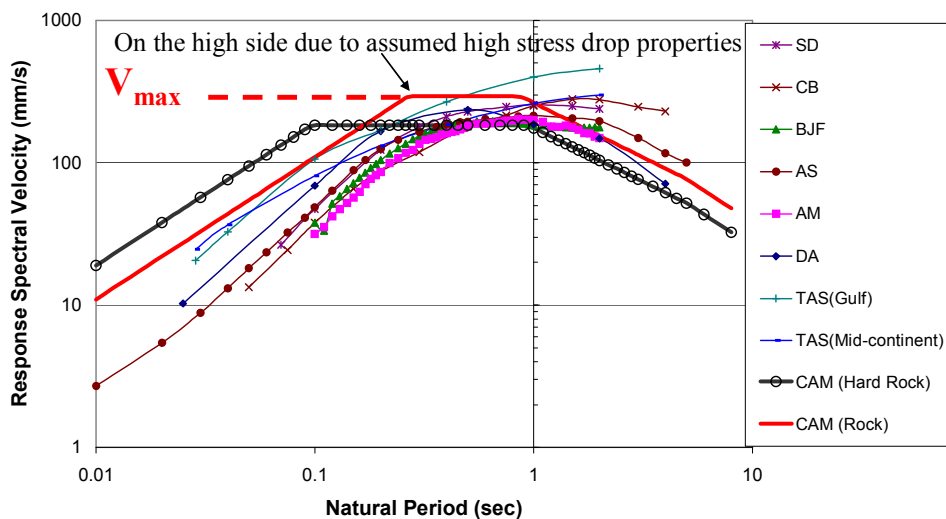
Fig. 2. Use of capacity spectrum for modelling collapse and overturning

The *Component Attenuation Model (CAM)* is an innovative framework by which the velocity and displacement demand on SDOF systems are expressed as product of component factors representing conditions of the source, path, local and site. The source factor is generic and hence used across different regions. Other factors that represent the path and local effects can be estimated in accordance with geophysical information of the region. The attenuation relationship is obtained by combining the generic source factor with the area specific factors. Further details of the CAM factors can be found in Sections 3 and 4.

It is shown in the velocity response spectrum of Fig. 3 that predictions of the spectral values by different empirical attenuation models can be highly variable and particularly in the low period range. Clearly, there is much less variability in the estimation of V_{max} in the median period range of 0.5s - 1.0s than that of A_{max} in the lower period range. Predictions by the whole range of attenuation models for the highest point on the velocity spectrum are

conservatively represented by the *Component Attenuation Model (CAM)* for rock conditions. The displacement demand behaviour of the earthquake in the high period range is also well constrained by the earthquake magnitude (and hence *seismic moment*). The apparent variability displayed in the high period (low frequency) range by certain models in Fig. 3 is only reflective of the poor resolution of the recorded data and not in the ground motions itself. Thus, the viability of generalising the predictions of the response spectrum parameters (V_{max} and D_{max}) is well demonstrated. Consequently, CAM is formulated to provide estimates for these demand parameters.

Comparison of Response Spectra from Different Attenuation Models



SD	Sadigh <i>et al.</i>	1997
CB	Campbell (Geomatrix)	1997
BJF	Boore, Joyner & Fumal	1997
AS	Abrahamson & Silva	1997
AM	Ambraseys	1995
DA	Dahle <i>et al.</i>	1990
TAS	Toro, Abrahamson & Schneider	1997
CAM	Component Attenuation Model (Lam <i>et al.</i>)	2000b

Fig. 3. Comparison of response spectra from different attenuation relationships (M7 R=30km on rock)

3. Formulation of the Component Attenuation Model

The Component Attenuation Model which comprises a number of component factors for estimation of the maximum velocity and displacement demand (V_{max} and D_{max}) is represented diagrammatically in Figure 4 and Equations (1) - (10).

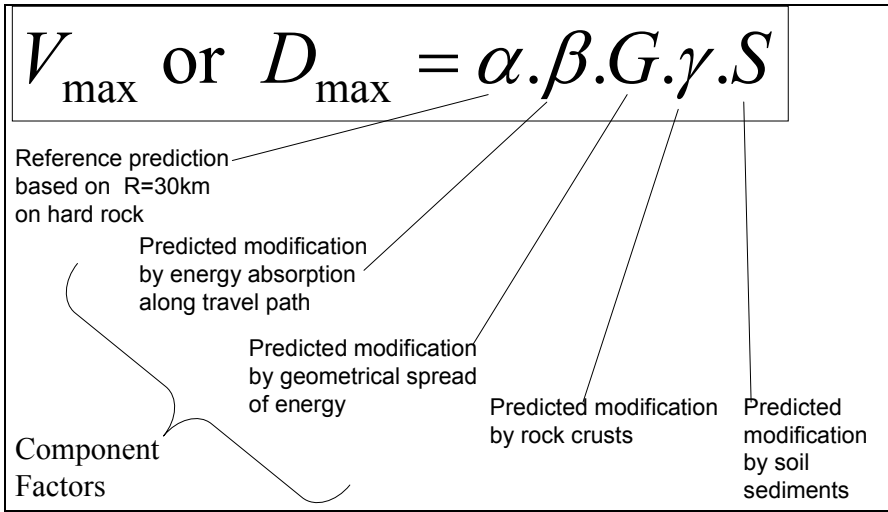


Fig. 4. Use of capacity spectrum for modelling collapse and overturning

Predictions of V_{\max}

$$V_{\max} = \alpha_V \cdot G \cdot \beta_V \cdot \gamma_V \cdot S \tag{1}$$

where

$$\alpha_V = 70 \{ 0.35 + 0.65(M - 5)^{1.8} \} \quad M \text{ is moment magnitude} \tag{2}$$

$$\beta_V = \left(\frac{30}{R} \right)^{0.005R} \quad R \text{ in km for } R < 50\text{km} \tag{3}$$

$$G = \frac{30}{R} \quad R \text{ in km for } R < 50\text{km} \tag{4}$$

γ_V is crustal factor

(value is typically in the range 1.6 - 2.0 but could be much lower in continental "shield" areas)

S is site factor (value is typically in the range 1.5 - 2.0 for average site)

Predictions of D_{\max}

$$D_{\max} = \alpha_D \cdot G \cdot \beta_D \cdot \gamma_D \cdot S \tag{5}$$

where

$$\alpha_D = \alpha_V \left(\frac{T_2}{2\pi} \right); \tag{6}$$

$$T_2 = 0.5 + \left(\frac{M - 5}{2} \right) \quad \text{for } M \leq 8 \quad (\text{Lam et al., 2000b}); \tag{7}$$

$$\text{or } \alpha_D = 10^{M-5} \quad \text{for } M \leq 6.5 \quad (\text{Lam \& Chandler, 2004}); \tag{8}$$

$$\beta_D = \left(\frac{30}{R} \right)^{0.003R} \quad R \text{ in km for } R < 50\text{km}; \tag{9}$$

$$G = \frac{30}{R} \quad R \text{ in km for } R < 50\text{km}; \tag{10}$$

γ_D is crustal factor

(value is typically in the order of 1.5-1.6 but could be much lower in continental "shield" areas)

S is site factor (value is typically in the range 1.5-2.0 for average site)

4. The Component Factors

4.1 The α_V and α_D factors

The component factors α_V and α_D as defined by equations (2) and (6-8) are for predicting the values of the V_{max} and D_{max} parameters at a reference distance of 30km (Lam *et al.*, 2000b). These equations were obtained from ensemble average response spectra that were simulated in accordance with the seismological source model of Atkinson (1993). The alternative expression of equation (8) for calculation of the value of α_D was derived from a theoretical approach presented by Lam and Chandler (2005). Predictions for the value of α_D from both approaches are very consistent for $M < 6.5$. For higher moment magnitude, equations (6-7) provide less conservative predictions. Ground motions so simulated have been scaled to a reference distance of 30 km as opposed to the usual 1km. This reference distance value is unique to CAM and is based on conditions of low and moderate seismicity which is characterised by moderate ground shaking with return periods of 500 – 2500 years.

4.2 The β_V and β_D factors

The component factors β_V and β_D are representing reduction in the seismic demand as the result of energy dissipation along the wave travel path. The effects of this form of attenuation, which are known as anelastic attenuation, are only significant to the prediction of the value of the V_{max} and D_{max} parameters at long distances. Thus, simple expressions like equations (3) and (9) have been used to represent its effects at close distances of $R < 50$ km. At longer distances, the determination of the β_V and β_D factors are expressed as functions of the Quality factor (Q_0) at a reference frequency of 1 hertz. The effects the value of Q_0 have upon the rate of wave attenuation is shown in the schematic diagram of Figure 5. Clearly, the higher the value of Q_0 , the better the wave transmission quality of the earth crust. Seismically active regions of young geological formations such as California have the value of Q_0 in the order of 100 – 200. Regions of ancient geological formation (intercontinental shield regions) such as *Central and Eastern North America* and parts of *Central and Western Australia* have the value of Q_0 typically exceeding 500.

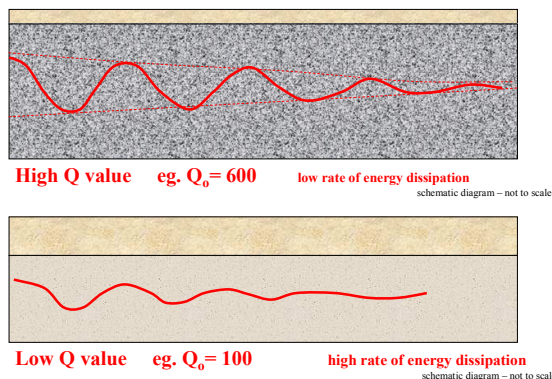


Fig. 5. Schematic representation of the effects of Quality factor on energy dissipation.

In a study by Chandler and Lam (2004) on the attenuation of long distance earthquakes, expressions defining the value of β_V and β_D (ie. rate of decrease in the values of the V_{max} and D_{max} parameters) as function of Q_0 and R have been derived from stochastic simulations of the seismological model. Functions defining the value of β_D is represented graphically by Fig.6 whilst values of β_V can be estimated using equation (11) once the value of β_D has been identified. It is noted that Fig. 6 is restricted to earthquakes with moment magnitude not exceeding 8. The attenuation modelling of ($M > 8$) mega magnitude earthquakes like the subduction earthquakes generated from off-shore of Sumatra would involve stochastic simulations of the seismological model (Lam *et al.*, 2009) and is beyond the scope of this book chapter.

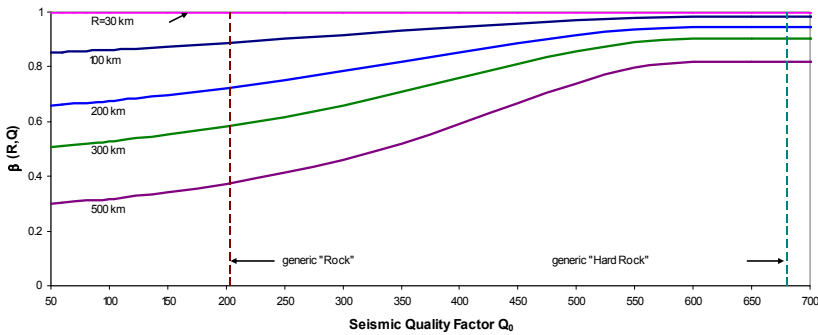


Fig. 6. Chart for determination of the value of β_D as function of Q_0 and R

$$\beta_V \approx 0.8\beta_D \quad \text{for} \quad R = 100km \quad (11a)$$

$$\beta_V \approx 0.6\beta_D \quad \text{for} \quad R = 200km \quad (11b)$$

$$\beta_V \approx 0.4\beta_D \text{ or } 0.5\beta_D \quad \text{for} \quad R = 300km \quad (11c)$$

4.3 The G factor

The G factor represents the effects of the geometrical spread of energy in space as seismic waves are radiated from a point source at the depth of rupture within the earth’s crust. At close range to the point source ($R < 50km$), spherical attenuation applies. The intensity of wave energy decreases in proportion to $1/R^2$ (as area of the surface of a sphere is proportional to the square of its radius). The rate of attenuation of the *Fourier* amplitude of the simulated wave is accordingly proportional to $1/R$ which is consistent with equations (4) and (10). The geometrical attenuation of seismic waves becomes more complex when the value of R is sufficiently large that reflection of waves from the Moho discontinuity and the associated wave-guide effects as shown in Figure 7 needs be taken into account. Thus, the depth of earth crust D in the region (ie. depth to the reflective surface of Moho) is an important modelling parameter. The value of D on land typically varies between 30 km and 60 km. Higher values are found in mountainous regions. Spherical attenuation may be assumed in the range $R < 1.5D$ and cylindrical attenuation in the range $R > 2.5D$ according to Atkinson & Boore (1995). Functions defining the value of the G factor for different values of D in the long distance range are represented graphically by Fig.8.

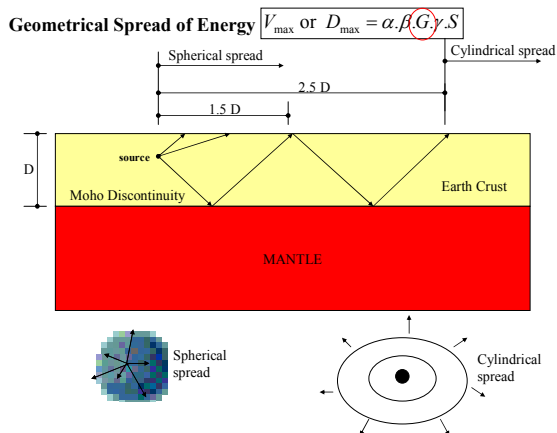


Fig. 7. Schematic representation of geometrical attenuation

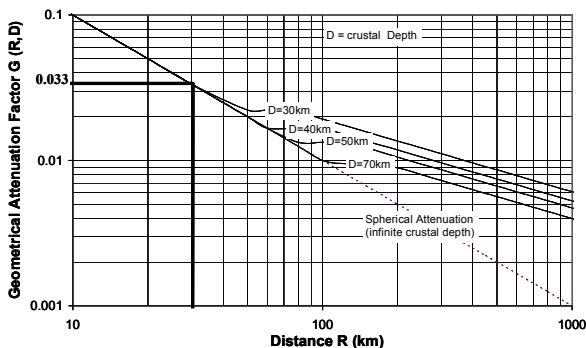


Fig. 8. G factor expressed as function of distance (R) and crustal depth (D)

4.4 The γ_V and γ_D factors

The crustal factor represents effects of modifications to the seismic waves as they propagate up the (rock) crust, and are made up of two components: (i) mid-crustal amplification and (ii) upper crustal modifications.

The amplitude of seismic waves generated at the source of the earthquake is proportional to the shear wave velocity of the earth crusts surrounding the fault rupture raised to the power of 3 (Atkinson & Silva, 1997). The α_V and α_D factors as described in Section 4.1 are both based on shear wave velocity of 3.8 km/s which is representative of conditions of the fault source at depths exceeding 12 km. For most moderate and large magnitude shallow earthquakes of $M \geq 6$, the centroid of the ruptured surface is constrained to a depth of around 5 km if the rupture area is of the order of 100 km² or larger. In this depth range, the shear wave velocity is estimated to average at around 3.5 km/s based on models presented by Boore and Joyner (1997). The mid-crustal factor is accordingly equal to 1.3 (being 3.8/3.5 raised to the power of 3).

Upward propagating seismic shear waves can be modified rapidly by the upper 1-2 km of the earth's crust shortly before the wave fronts reaches the ground surface. Much is attributed to the shear wave velocity gradient of the crustal medium. Meanwhile, seismic waves could also be attenuated fairly rapidly through energy dissipation by the typically highly fissured rocks in the upper 3-4 km of the earth's crust. These path effects can be difficult to track if measurements have only been taken from the ground surface. Upper crustal modifications were well demonstrated by the study of Abercrombie (1997) in which seismometer records collected from several km deep boreholes were analysed. Stochastic simulations undertaken the authors based on the generic *rock* profile of Boore and Joyner (1997) and principles of *quarter wave-length method* for the calculation of frequency dependent amplification revealed an upper crustal factor of about 1.2 (Lam *et al.*, 2000b) when co-existing attenuation in the upper crust (based on parameters that are consistent with strong ground shaking in active regions like California) had also been taken into account. The attenuation parameter that can be used to characterised upper crustal attenuation is known as *Kappa* (Anderson & Hough, 1984). The value of this parameter for strong ground shaking in generic *rock* is in order of 0.04 - 0.07 (Atkinson & Silva, 1997; Atkinson & Boore, 1998; Tsang & Lam, 2010). For conditions of moderate ground shaking and in regions of older geological formation (which is characterised by a lower *Kappa* value of the order of 0.02-0.03) a higher upper crustal factor of 1.5 in the velocity controlled region of the response spectrum is estimated (Lam & Wilson, 2004). Behaviour of amplification in the displacement controlled region of the response spectrum is more robust and is insensitive to the *Kappa* value.

In summary, the combined crustal factor γ_V for modelling the velocity demand (V_{max}) is accordingly in the range 1.5 - 2.0 (based on the product of "1.3" and "1.2 - 1.5") depending on the intensity of ground shaking and type geological formation, whilst the combined crustal factor γ_D for modelling the displacement demand (D_{max}) is in the order of 1.5 - 1.6. However, much lower values of γ_V or γ_D should be assumed for continental "shield" areas where there are much less modifications of the upward propagating waves by the very hard rock in those areas.

These crustal factor values can be compared with the ratio of ground shaking estimated in regions of very different geological formation but of the same earthquake scenario and source processes. The inferred ratio of ground shaking between *Western Australia* and *Southeastern Australia* has been found to be 1.5 - 1.7 based on the Intensity model of Gaull *et al.* (1990) developed for both regions. Similarly, the inferred ratio of ground shaking between the mid-continental region of *Central and Eastern North America* and that of *Mexican Gulf* (of younger geological formations) has been found to be 1.5 - 1.6 based on the stochastic model of Toro *et al.* (1997). The inferred ratio between *Western North American* and *Central and Eastern North America* has been found to be in between 1.3 - 1.8 based on the stochastic model of Atkinson and Silva (2000). These inferred ratios are all in broad agreement with the values of the γ_V and γ_D factors that have been recommended by CAM.

Recommendations that have been made in the above enable quick estimates of the response spectrum parameters to be made whilst alleviating the need for any rigorous analysis of strong motion or seismological data. Precise evaluation of the crustal factors would involve

measuring and modelling the shear wave velocity gradient of the earth crusts in the region (Chandler *et al.*, 2005a & 2006a; Lam *et al.*, 2006; Tsang *et al.*, 2010), constraining $Kappa$ values either by analysis of *Coda Wave* data or by making use of generic correlations between values of $Kappa$ and shear wave velocity parameters of the earth's crust in the region (Chandler *et al.*, 2005b & 2006b), and calculating filter functions that take into account both the amplification and attenuation effects. Stochastic simulations of the seismological model that have incorporated these developed filter functions can provide direct estimates of the crustal effects on ground shaking in projected earthquake scenarios. However, it is beyond the scope of this book chapter to present details of these modelling processes.

5. Comparison with recorded data and examples

The *Component Attenuation Model* as described is essentially a tool for providing estimates of the response spectrum parameters for rock outcrops. Meanwhile, velocity parameters of ground shaking on average sites can be inferred from Intensity data collected from historical earthquake events. Comparisons of the two sets of data provide estimates of the site factors that represent the difference between ground shaking on rock and that on an average site in pre-determined earthquake scenarios. This calibration process for constraining the site factor is illustrated in the schematic diagram of Figure 9.

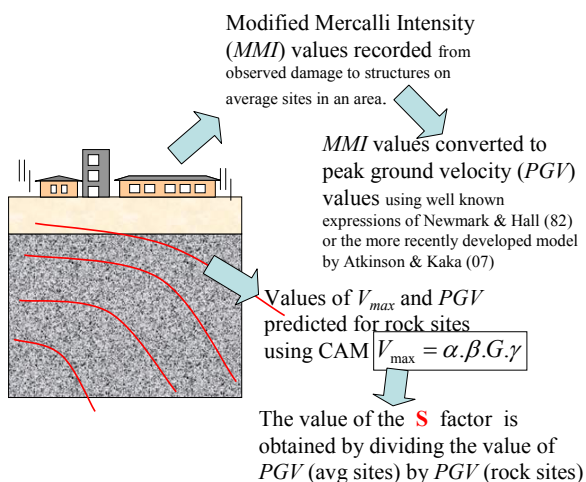


Fig. 9. Inferring Site factor

Using this calibration approach, the value of S factor for average sites have been found to be 1.5 – 1.8 in a study undertaken for three regions within Central China (Tsang *et al.*, 2010); 1.5 for Australia on average (Lam *et al.*, 2003); 1.7 for Northern Iran (Yaghmaei-Sabegh and Lam, 2010); and a slightly higher value of about 2.0 for the South China region surrounding Hong Kong. Importantly, this range of calibrated site factors obtained from different studies are in broad agreement and consistent with the site factor recommended by *NEHRP* for common shallow soil sites.

Further evaluation of the CAM expressions have been undertaken by Lumantarna et al. (2010) based on comparing response spectrum parameters calculated from the CAM expressions presented in this book chapter and those calculated from some 196 accelerogram records that were made available from data resources provided online by the Pacific Earthquake Engineering Research Centre (PEER). This database of strong motion accelerograms were mainly made up of records taken from California and with a few records from Southern Europe (Italy) and from Turkey. These records which were mainly post 1980 (except for a few taken in the 1970's) were all recorded on Class B sites (soft rock and stiff soil) with shear wave velocity in the range 360 - 750 m/s and from events of magnitude M5 - M7 within epicentral distances 50 - 60 km and thus within the scope of the presented CAM expressions. CAM was then applied using the expressions outlined in Section 3, with $\gamma = 1.5$ and $S = 1.5$ in view of the conditions of strong ground shaking in most of the recorded events. It is shown in the comparative plots of Figs. 10 - 11 that CAM generally provides a conservative estimate for the V_{max} and D_{max} values although a large scatter exists. It is important to note that few recorded results exceed 2 times the CAM estimates with less scatter with the recorded values of D_{max} .

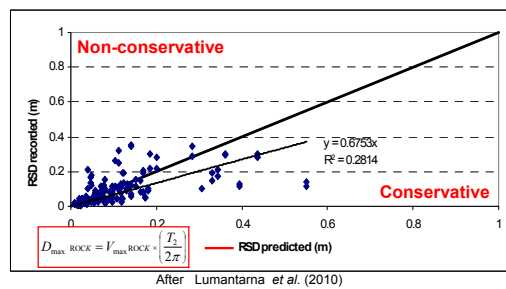
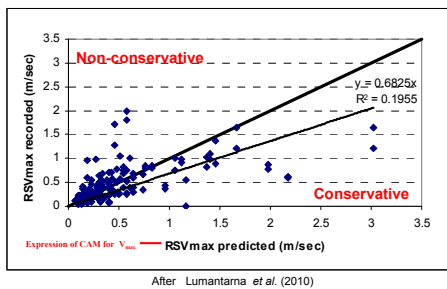


Fig. 10. Recorded and Predicted V_{max} values

Fig. 11. Recorded and Predicted D_{max} values

6. Examples for illustrating the use of CAM

Finally, the use of the CAM expressions for estimating the value of V_{max} and D_{max} are illustrated with two examples: (i) M5.6 event at a distance of 16km and (ii) M7 event at a distance of 100 km. Both earthquake scenarios are assumed to occur in the young geological (sandstone) formation of the Sydney basin. Crustal depth D can be taken as 30 km and value of Q_0 is 200. Example 1 was a real event that occurred in the City of Newcastle in December 1989, but no accelerogram records exist of that event.

6.1 Example 1

Input data is $M=5.6$, $R=16$ km

$$V_{\max} = \alpha_V \cdot G \cdot \beta_V \cdot \gamma_V \cdot S \tag{12}$$

where

$$\alpha_V = 70 \{0.35 + 0.65(M - 5)^{1.8}\} = 70 \{0.35 + 0.65(5.6 - 5)^{1.8}\} = 43 \text{ mm/s} \tag{13}$$

$$\beta_V = \left(\frac{30}{R}\right)^{0.005R} = \left(\frac{30}{16}\right)^{0.005 \times 16} = 1.05 \tag{14}$$

$$G = \frac{30}{R} = \frac{30}{16} = 1.9 \tag{15}$$

$$\gamma_V = 1.6$$

$$S = 1.5 \text{ for average site} \tag{16}$$

$$V_{\max} = (43 \text{ mm/s})(1.9)(1.05)(1.6)(1.5) = 205 \text{ mm/s} \tag{17}$$

$$D_{\max} = \alpha_D \cdot G \cdot \beta_D \cdot \gamma_D \cdot S \tag{18}$$

where

$$\alpha_D = \alpha_V \left(\frac{T_2}{2\pi}\right) = 43 \times \left(\frac{0.8}{2\pi}\right) = 5.5 \text{ mm} \tag{19}$$

$$T_2 = 0.5 + \left(\frac{M - 5}{2}\right) = 0.5 + \left(\frac{5.6 - 5}{2}\right) = 0.8 \text{ s} \tag{20}$$

$$\beta_D = \left(\frac{30}{R}\right)^{0.003R} = \left(\frac{30}{16}\right)^{0.003 \times 16} = 1.03 \tag{21}$$

$$G = \frac{30}{R} = \frac{30}{16} = 1.9 \tag{22}$$

$$\gamma_D = S = 1.5 \tag{23}$$

$$D_{\max} = (5.5 \text{ mm})(1.9)(1.03)(1.5)(1.5) = 24 \text{ mm} \tag{24}$$

Response spectra of two different formats constructed in accordance with the calculated values of V_{\max} and D_{\max} are shown in Fig. 12 in below.

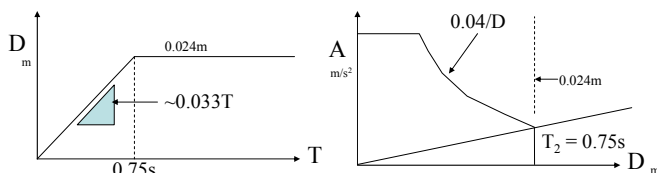


Fig. 12. Response spectra constructed for example 1

6.2 Example 2

Input data is $M=7$, $R=100$ km, $D=30$ km and $Q_0 = 200$

$$V_{\max} = \alpha_V \cdot G \cdot \beta_V \cdot \gamma_V \cdot S \tag{25}$$

$$\alpha_V = 70 \{0.35 + 0.65(M - 5)^{1.8}\} = 70 \{0.35 + 0.65(7 - 5)^{1.8}\} = 180 \text{ mm/s} \tag{26}$$

$$G = \frac{0.02}{0.033} = 0.6 \text{ as indicated by chart in Fig. 13 below} \tag{27}$$

$$\beta_V = 0.9 \text{ as indicated by the chart in Fig. 14 below; } \beta_V \approx 0.8 \beta_D \approx 0.7$$

$$V_{\max} = 180 \text{ mm/s}(0.6)(0.7)(1.5)(1.5) \approx 170 \text{ mm/s} \tag{28}$$

$$\alpha_D = \alpha_V \left(\frac{T_2}{2\pi}\right) = \alpha_V \left(\frac{0.5 + \left(\frac{M-5}{2}\right)}{2\pi}\right) = 180 \left(\frac{0.5 + \left(\frac{7-5}{2}\right)}{2\pi}\right) = 180 \left(\frac{1.5}{2\pi}\right) = 43 \text{ mm} \tag{29}$$

$$D_{\max} = 43 \text{ mm}(0.6)(0.9)(1.5)(1.5) \approx 55 \text{ mm} \tag{30}$$

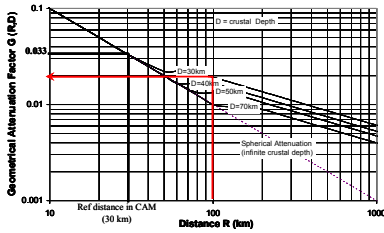


Fig. 13. Identification of the value of G

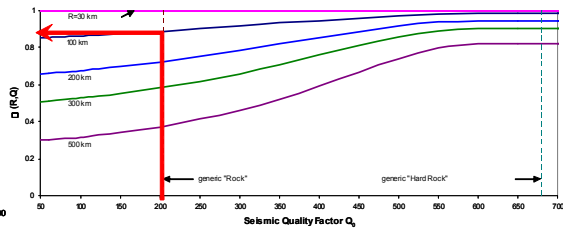


Fig. 14. Identification of the value of β_D

Response spectra of two different formats constructed in accordance with the calculated values of V_{max} and D_{max} for the distant earthquakes are shown in Fig. 15 in below. It is noted that the corner period (T_2) of 1.5s in the source factor has been increased to 2s by the long distance (path) effects which are represented by the β_V and β_D factors.

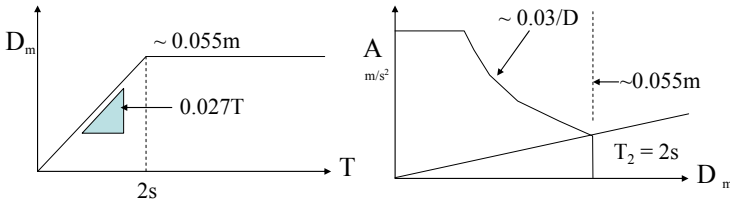


Fig. 15. Response spectra constructed for Example 2

7. Conclusions

This paper introduces the *Component Attenuation Model (CAM)* which is a generalised attenuation model that has been derived from stochastic simulations of the seismological model. The model is made up of a series of component factors representing the effects of the source, the wave travel path, modifications by the earth's crust and that of the site. Expressions and charts have been presented for evaluation of the individual factors. Parameter values calculated by the CAM expressions have been compared with those calculated from some 196 recorded accelerograms obtained from the PEER database. Two examples illustrating the use of CAM have been shown.

8. References

Abercrombie, R.E. (1997), Near-surface attenuation and site effects from comparison of surface and deep borehole recording, *Bulletin of the Seismological Society of America*, Vol.87: 731-744.

Abrahamson, N.A. & Silva, W.J. (1997), Empirical response spectral attenuation relations for shallow crustal earthquakes, *Seismological Research Letters*, Vol. 68(No.1): 94-127.

Ambraseys, N.N. (1995), The prediction of earthquake peak ground acceleration in Europe. *Earthquake Engineering & Structural Dynamics*, Vol. 24: 467-490.

- Anderson, J.G. & Hough, S.E. (1984), A Model for the Shape of the Fourier Amplitude Spectrum of Acceleration at High Frequencies, *Bulletin of the Seismological Society of America*, Vol.74 (No.5): 1969-1993.
- Atkinson, G.M. (1993), Earthquake source spectra in Eastern North America. *Bulletin of the Seismological Society of America*, Vol.83: 1778-1798.
- Atkinson, G.M. & Boore, D.M. (1995), Ground-motion relations for Eastern North America. *Bulletin of the Seismological Society of America*, Vol.85 (No.1): 17-30.
- Atkinson, G.M. & Silva, W. (1997), An empirical study of earthquake source spectra for Californian earthquakes, *Bulletin of the Seismological Society of America*, Vol.87: 97-113.
- Atkinson, G.M. & Boore, D.M. (1998), Evaluation of models for earthquake source spectra in Eastern North America. *Bulletin of the Seismological Society of America*, Vol.88(No.4): 917-937.
- Atkinson, G.M. & Silva, W. (2000), Stochastic modeling of Californian Ground Motions, *Bulletin of the Seismological Society of America*, Vol.90: 255-274.
- Atkinson, G. M. & S. I. Kaka (2007), Relationship between Felt Intensity and Instrumental Ground motion in the Central United State and California. *Bulletin of the Seismological Society of America*, Vol.97 (No.2): 497-510.
- Balendra, T., Lam, N.T.K., Wilson, J.L. & Kong, K.H. (2001), Analysis of long-distance earthquake tremors and base shear demand for buildings in Singapore, *Journal of Engineering Structures*. Vol.24: 99-108.
- Boore, D.M. (1983), Stochastic Simulation of high-frequency ground motions based on seismological model of the radiated spectra, *Bulletin of the American Seismological Society of America*, Vol.73 (No.6): 1865-1894.
- Boore, D.M. & Joyner, W.B. (1997), Site amplifications for generic rock sites, *Bulletin of the Seismological Society of America*, Vol.87 (No.2): 327-341.
- Boore, D.M., Joyner, W.B. & Fumal, T.E. (1997), Equations for estimating horizontal response spectra and peak acceleration for western North American earthquakes: a summary of recent work, *Seismological Research Letters*, Vol.68: 128-153.
- Brune, J.N. (1970), Tectonic stress and the spectra of seismic shear waves from earthquakes, *Journal of Geophysics Research*, Vol.75: 4997-5009.
- Campbell, K.W. (1997), Empirical near-source attenuation relationships for horizontal and vertical components of peak ground acceleration, peak ground velocity, and pseudo-absolute acceleration response spectra, *Seismological Research Letters*, Vol.68 (No.1): 154-179.
- Chandler, A.M. & Lam, N.T.K. (2002), Intensity Attenuation Relationship for the South China Region and Comparison with the Component Attenuation Model, *Journal of Asian Earth Sciences*. Vol.20: 775-790.
- Chandler, A.M. & Lam, N.T.K. (2004), An attenuation model for distant earthquakes, *Earthquake Engineering and Structural Dynamics*. Vol.33 (No.2): 183-210.
- Chandler, A.M., Lam, N.T.K., & Tsang, H.H. (2005a), Shear Wave Velocity Modelling in Bedrock for Analysis of Intraplate Seismic Hazard, *Journal of Soil Dynamics & Earthquake Engineering*. Vol.25: 167-185.
- Chandler, A.M., Lam, N.T.K., & Tsang, H.H.(2005b), Estimation of Near Surface Attenuation Parameter in Crustal Rock by Calibration Analyses, *International Journal of Seismology and Earthquake Engineering*. Vol. 7 (No.3): 159-172.

- Chandler, A.M., Lam, N.T.K., & Tsang, H.H. (2006a), Regional and Local Factors in Attenuation Modelling, *Journal of Asian Earth Sciences*. Vol.27: 892 - 906.
- Chandler, A.M., Lam, N.T.K., & Tsang, H.H. (2006b). Near Surface Attenuation Modelling based on Rock Shear Wave Velocity Profile. *Journal of Soil Dynamics & Earthquake Engineering*, Vol.26 (No.11): 1004-1014.
- Gaull, B.A., Michael-Leiba, M.O. & Rynn, J.M.W. (1990), Probabilistic earthquake risk maps of Australia, *Australian Journal of Earth Sciences*, Vol.37: 169-187.
- Hutchinson, G.L., Lam, N.T.K. & Wilson, J.L. (2003), Determination of earthquake loading and seismic performance in intraplate regions, *Progress in Structural Engineering and Materials*, 2003. Vol.5: 181-194.
- Lam, N.T.K., Wilson, J.L. & Hutchinson, G.L. (2000a), Generation of Synthetic Earthquake Accelerograms Using Seismological Modelling : A Review, *Journal of Earthquake Engineering* , Vol.4(No.3): 321-354.
- Lam, N.T.K., Wilson, J.L., Chandler, A.M. and Hutchinson, G.L. (2000b), Response Spectral Relationships for Rock Sites Derived from The Component Attenuation Mode, *Earthquake Engineering and Structural Dynamics*, Vol.29 (No.10): 1457-1490.
- Lam, N.T.K., Wilson, J.L., Chandler, A.M. and Hutchinson, G.L. (2000c), Response Spectrum Modelling for Rock Sites in Low and Moderate Seismicity Regions Combining Velocity, Displacement and Acceleration Predictions, *Earthquake Engineering and Structural Dynamics*, Vol.29 (No.10): 1491-1526.
- Lam, N.T.K., Wilson, J.L., Chandler, A.M. & Hutchinson, G.L.(2002), Response Spectrum Predictions for Potential Near-Field and Far-Field Earthquakes Affecting Hong Kong : Rock Sites. *Soil Dynamics and Earthquake Engineering*. Vol.22: 47-72.
- Lam, N.T.K., Sinadinovski, V., Koo, R.C.H. & Wilson, J.L.(2003), Peak Ground Velocity Modelling for Australian Intraplate Earthquakes. *International Journal of Seismology and Earthquake Engineering*. Vol.5(No.2): 11-22.
- Lam, N.T.K. & Wilson, J.L.(2004), Displacement Modelling of Intraplate Earthquakes, special issue on Performance Based Seismic Design, *International Seismology and Earthquake Technology Journal*, Vol.41 (No.1): 15-52.
- Lam, N.T.K. & Chandler, A.M.(2005). Peak Displacement Demand in Stable Continental Regions, *Earthquake Engineering and Structural Dynamics*. Vol.34: 1047-1072.
- Lam, N.T.K., Wilson, J.L. & Srikanth, V.(2005), Accelerograms for dynamic analysis under the New Australian Standard for Earthquake Actions, *Electronic Journal of Structural Engineering*. Vol.5: 10-35.
- Lam, N.T.K., Asten, M., Roberts, J., Srikanth, V., Wilson, J.L., Chandler, A.M. & Tsang, H.H. (2006), Generic Approach for Modelling Earthquake Hazard, *Journal of Advances in Structural Engineering*, Vol.9 (No.1): 67-82.
- Lam, N.T.K., Balendra, T., Wilson, J.L. & Srikanth, V. (2009), Seismic Load Estimates of Distant Subduction Earthquakes Affecting Singapore, *Engineering Structures*, Vol.31 (No.5): 1230-1240.
- Lumantarna, E., Lam, N.T.K. & Wilson, J.L. (2010), Studies of peak displacement demand and second corner period, *Report Infrastructure Group, Department of Civil & Environmental Engineering*.
- Newmark, N.M. & Hall, W.J. (1982) *Earthquake spectra and design*. EERI Monograph, Earthquake Engineering Research Institute, California, U.S.A.

- Priestley, M.J.N. (1995). Displacement-based seismic assessment of existing reinforced concrete buildings, *Procs. 5th Pacific Conf. on Earthquake Eng.*, Melbourne, 225-244.
- Sadigh, K., Chang, C.Y., Egan, J.A., Makdisi, F. & Youngs, R.R. (1997), Attenuation relationships for shallow crustal earthquakes based on Californian strong motion data, *Seismological Research Letters*, Vol.68 (No.1): 180-189.
- Toro, G.R., Abrahamson, N.A. & Schneider, J.F. (1997), Model of strong ground motions from earthquakes in Central and Eastern North America: best estimates and uncertainties. *Seismological Research Letters*, Vol.68 (No.1): 41-57.
- Tsang, H.H. & Lam, N.T.K. (2010), *Seismic Hazard Assessment in Regions of Low-to-Moderate Seismicity*, Lambert Academic Publishing, Deutsh. ISBN:978-3-8383-3685-5.
- Tsang, H.H., Sheikh, N. & Lam, N.T.K. (2010), Regional Differences in Attenuation Modelling for Eastern China, *Journal of Asian Earth Sciences*, Vol. 39(5): 441-459.
- Wilson, J.L. & Lam, N.T.K. (2003), A recommended earthquake response spectrum model for Australia, *Australian Journal of Structural Engineering*, Vol.5(No.1): 17-27.
- Yaghmaei-Sabegh, S & Lam, N.T.K. (2010). Ground motion modelling in Tehran based on the stochastic method, *Soil Dynamics and Earthquake Engineering*, Vol.30 : 525-535.



Stochastic Control

Edited by Chris Myers

ISBN 978-953-307-121-3

Hard cover, 650 pages

Publisher Sciyo

Published online 17, August, 2010

Published in print edition August, 2010

Uncertainty presents significant challenges in the reasoning about and controlling of complex dynamical systems. To address this challenge, numerous researchers are developing improved methods for stochastic analysis. This book presents a diverse collection of some of the latest research in this important area. In particular, this book gives an overview of some of the theoretical methods and tools for stochastic analysis, and it presents the applications of these methods to problems in systems theory, science, and economics.

How to reference

In order to correctly reference this scholarly work, feel free to copy and paste the following:

Nelson Lam, John Wilson and Hing Ho Tsang (2010). Modelling Earthquake Ground Motions by Stochastic Method, Stochastic Control, Chris Myers (Ed.), ISBN: 978-953-307-121-3, InTech, Available from: <http://www.intechopen.com/books/stochastic-control/modelling-earthquake-ground-motions-by-stochastic-method>

INTECH

open science | open minds

InTech Europe

University Campus STeP Ri
Slavka Krautzeka 83/A
51000 Rijeka, Croatia
Phone: +385 (51) 770 447
Fax: +385 (51) 686 166
www.intechopen.com

InTech China

Unit 405, Office Block, Hotel Equatorial Shanghai
No.65, Yan An Road (West), Shanghai, 200040, China
中国上海市延安西路65号上海国际贵都大饭店办公楼405单元
Phone: +86-21-62489820
Fax: +86-21-62489821

© 2010 The Author(s). Licensee IntechOpen. This chapter is distributed under the terms of the [Creative Commons Attribution-NonCommercial-ShareAlike-3.0 License](#), which permits use, distribution and reproduction for non-commercial purposes, provided the original is properly cited and derivative works building on this content are distributed under the same license.